Urban Floodwater Mapping From Aerial Imagery With Dense Shadows via Semi-Supervised Learning

Yongjun He, PhD Candidate

Dr. Jinfei Wang, Supervisor

Dr. Ying Zhang, Co-supervisor (NRCan)

Department of Geography and Environment

Western University

Western-ICLR Multi-hazard Risk and Resilience Workshop

Nov 3, 2022

Western UNIVERSITY · CANADA

Natural Resources Canada

Ressources naturelles Canada

NSERC CRSNG

Outline

- 1. Background
- 2. Research question
- 3. Methodology
- 4. Experiments and results
- 5. Conclusions

1. Background

- A growing number of flooding events with the increased intensity of climate change (Armenakis et al., 2017; Feng et al., 2015).
- More earth observation data available from various remotely sensed platforms (Ghaffarian et al., 2018).
- Floodwater mapping based on aerial imagery can offer timely information for emergency response and rescue operations in urban areas (Shen et al., 2019).

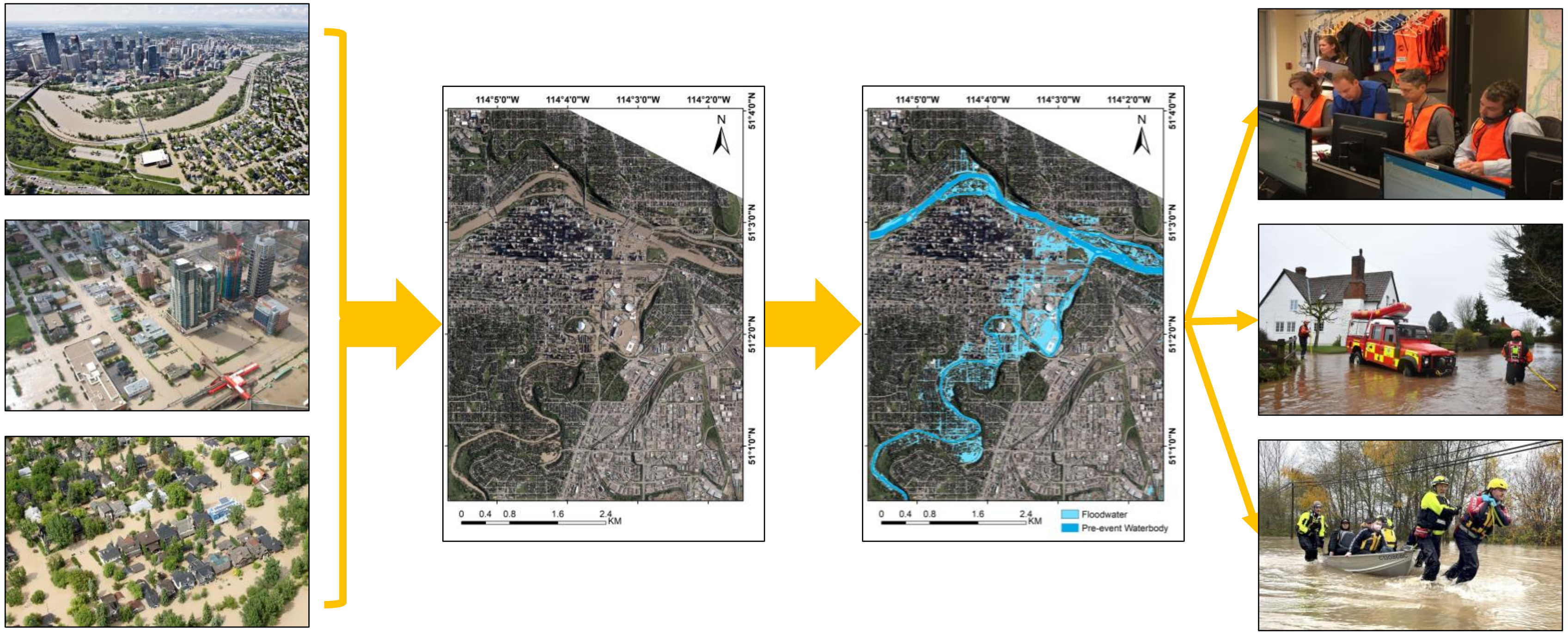

Urban flood | **Remote sensing Image** | **Flooding Map** | **Disaster Response**

1. Background

- **Floodwater mapping methods**
  - Spectral index methods
  - AI techniques
    - Traditional machine learning
    - Deep learning

➢ Spectral index methods

e.g., floodwater index (FWI) (Zhang & Crawford, 2020).

$$FWI = \frac{(B_r - B_b) + (B_r - B_g)}{100}$$

Advantage

Simple and fast deployment

Disadvantage

(1) Need more processing steps, such as image segmentation, spectral analysis

(2) Cannot extract the visible floodwater covered by shadows, which underestimates the flooding outcome in dense urban areas

Images	Extraction results w/o considering shadowed floodwater	Extraction results w/ considering shadowed floodwater

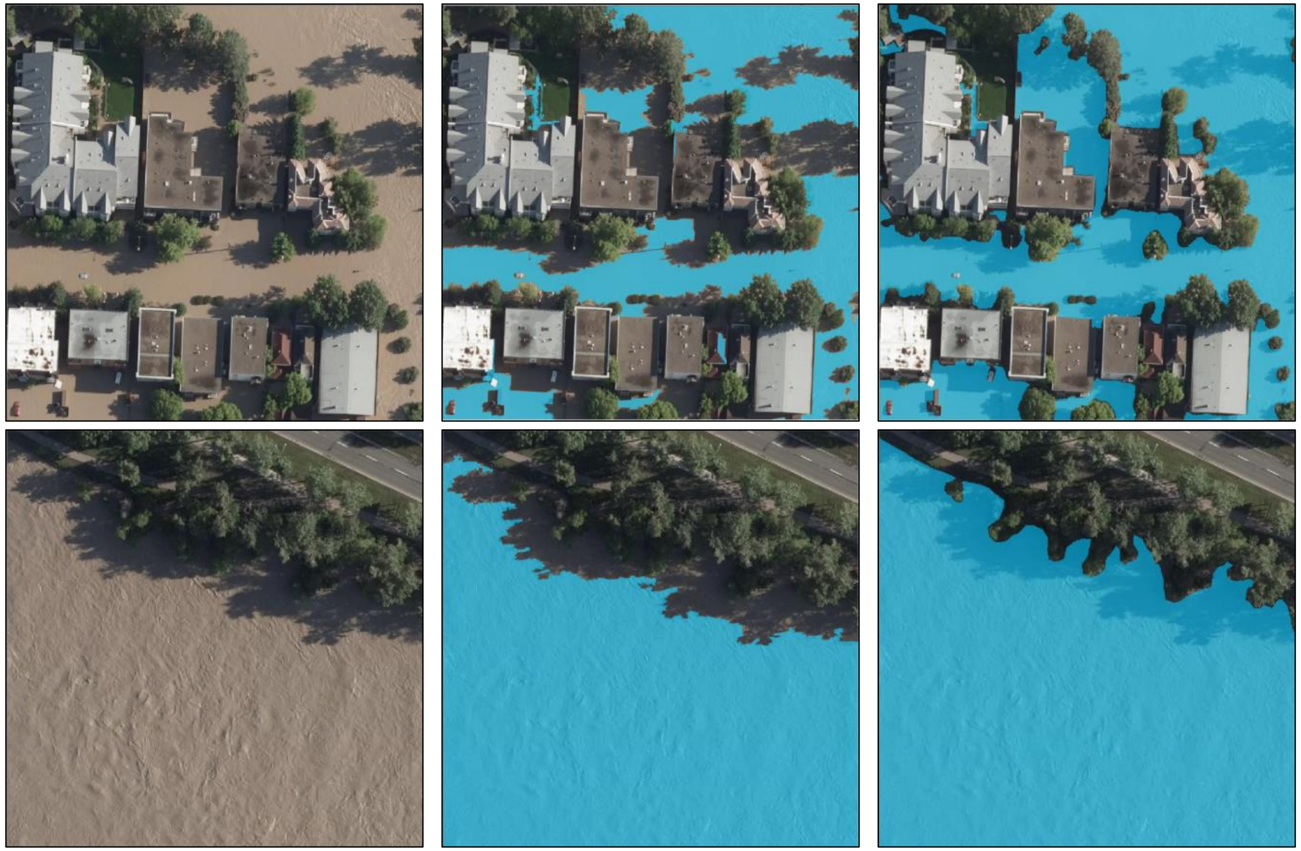

1. Background

- **Traditional machine learning**

  e.g., support vector machine, random forest, etc.
  Advantage
  (1) Only requiring a small number of training samples
  (2) Higher accuracy than spectral index method

  Disadvantage
  (1) Relying on manually designed features (e.g., spectrum, texture, and shape, etc.) with expert knowledge
  (2) Performance does not increase with training data size
  (3) Hard to design proper features to extract the floodwater in shadows

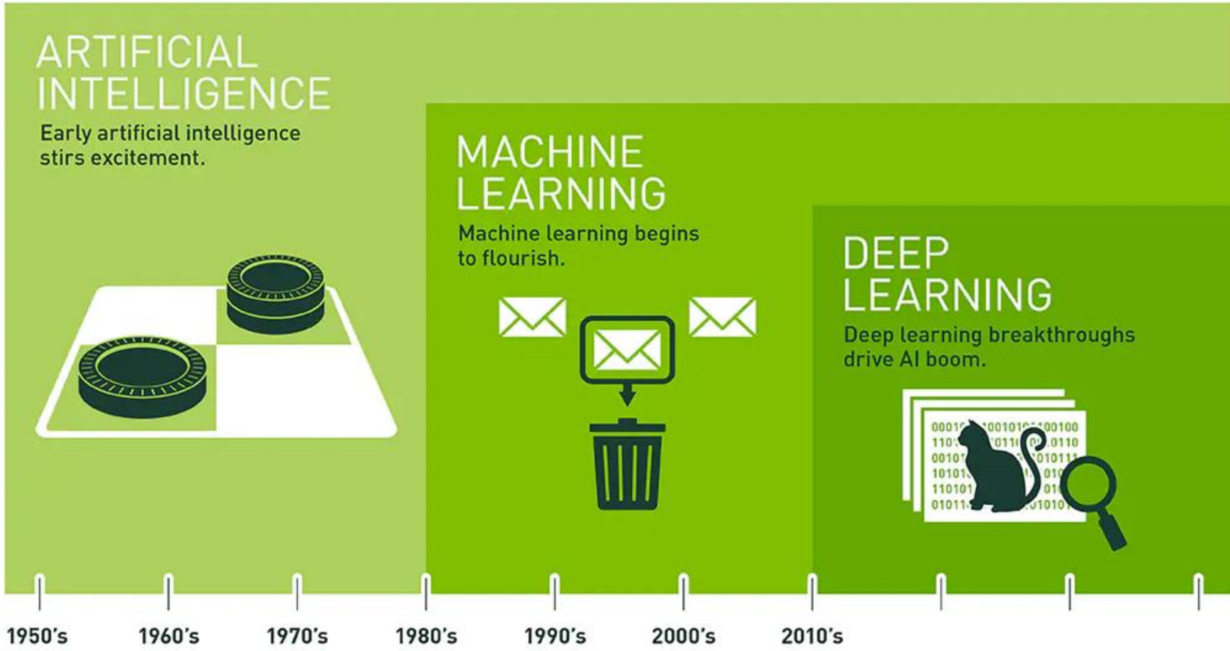

Since an early flush of optimism in the 1950s, smaller subsets of artificial intelligence – first machine learning, then deep learning, a subset of machine learning – have created ever larger disruptions.

- **Deep learning**

  e.g., convolutional neural networks (CNNs), etc.
  Advantage
  (1) Automatic feature extraction
  (2) The more training data, the better performance

  Disadvantage
  (1) Requiring huge computing resources
  (2) Requiring a large amount of labeled training data

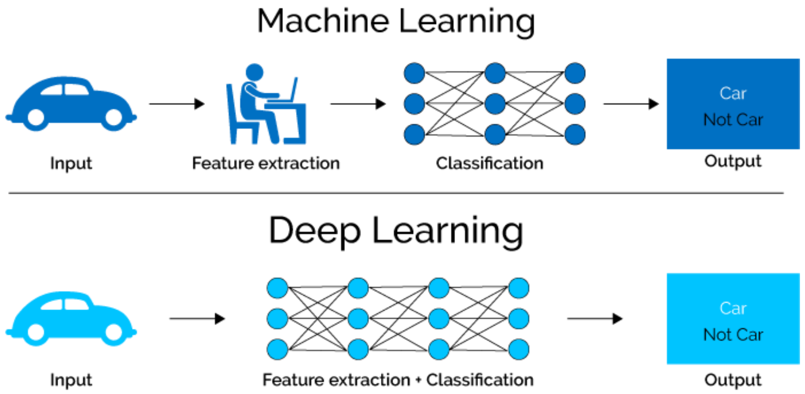

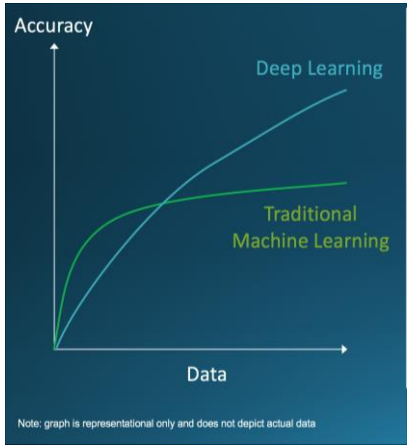

2. Research question

- **Existing issues**

(1) Spectral index and traditional machine learning methods cannot efficiently detect visible floodwater in shadows.
(2) Deep learning methods perform better than traditional methods. However, It is time-consuming to create a mass of labels for model building.

- **Research question?**

How can we extract the floodwater (including shadowed and non-shadowed) from the aerial imagery base on deep learning algorithm with a limited number of labeled samples?

3. Methodology

- **Semi-supervised learning**

  Incorporating a small number of labeled data and a large amounts of unlabeled data to determine a better decision boundary.

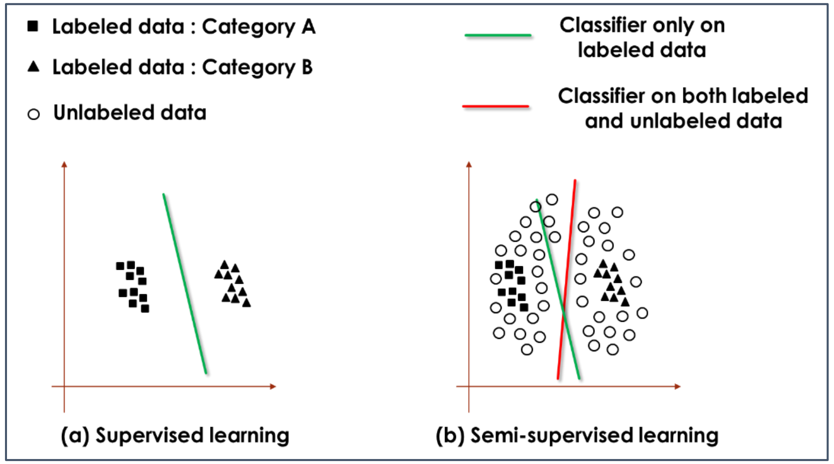

- **Consistency regularization** encourages the model to give consistent predictions for unlabeled inputs perturbed in different ways .
- **Loss function**:

$$\mathcal{L} = \mathcal{L}_s + \mathcal{L}_{Cons}$$

  $\mathcal{L}_s$ denotes the supervised loss.

  $\mathcal{L}_{Cons}$ denotes the consistency loss.

- **Why works?**

  The use of large amounts of unlabeled data can enlarge the training data distribution and help learn more hidden features to improve the model generalizability.
- **Advantages**

  A large number of unlabeled data can be utilized to improve the model performance when there are very few labels.

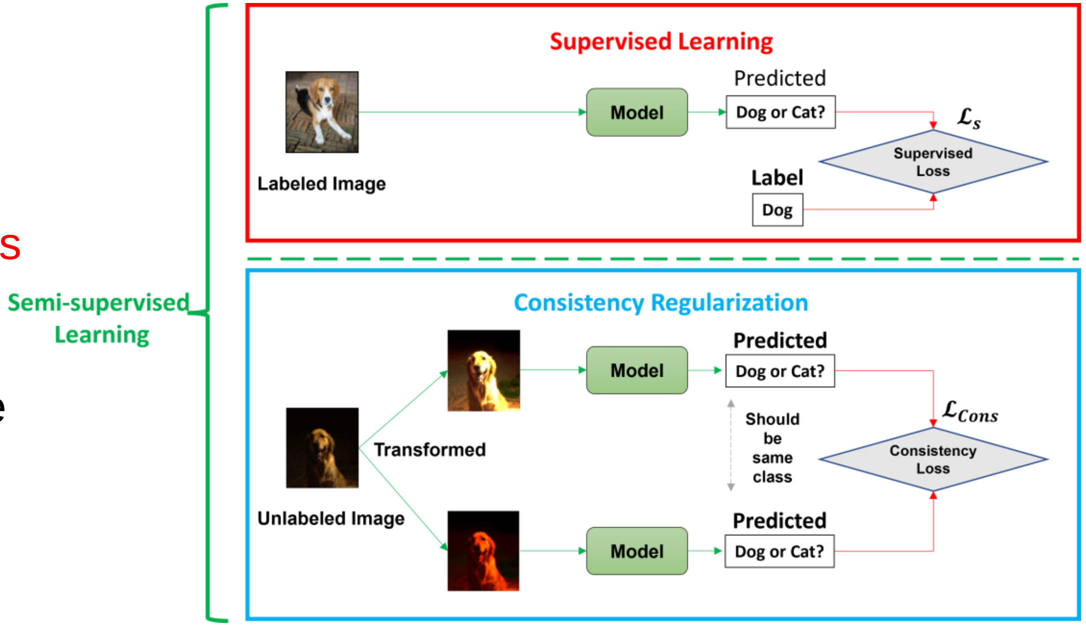

- **Proposed semi-supervised framework**

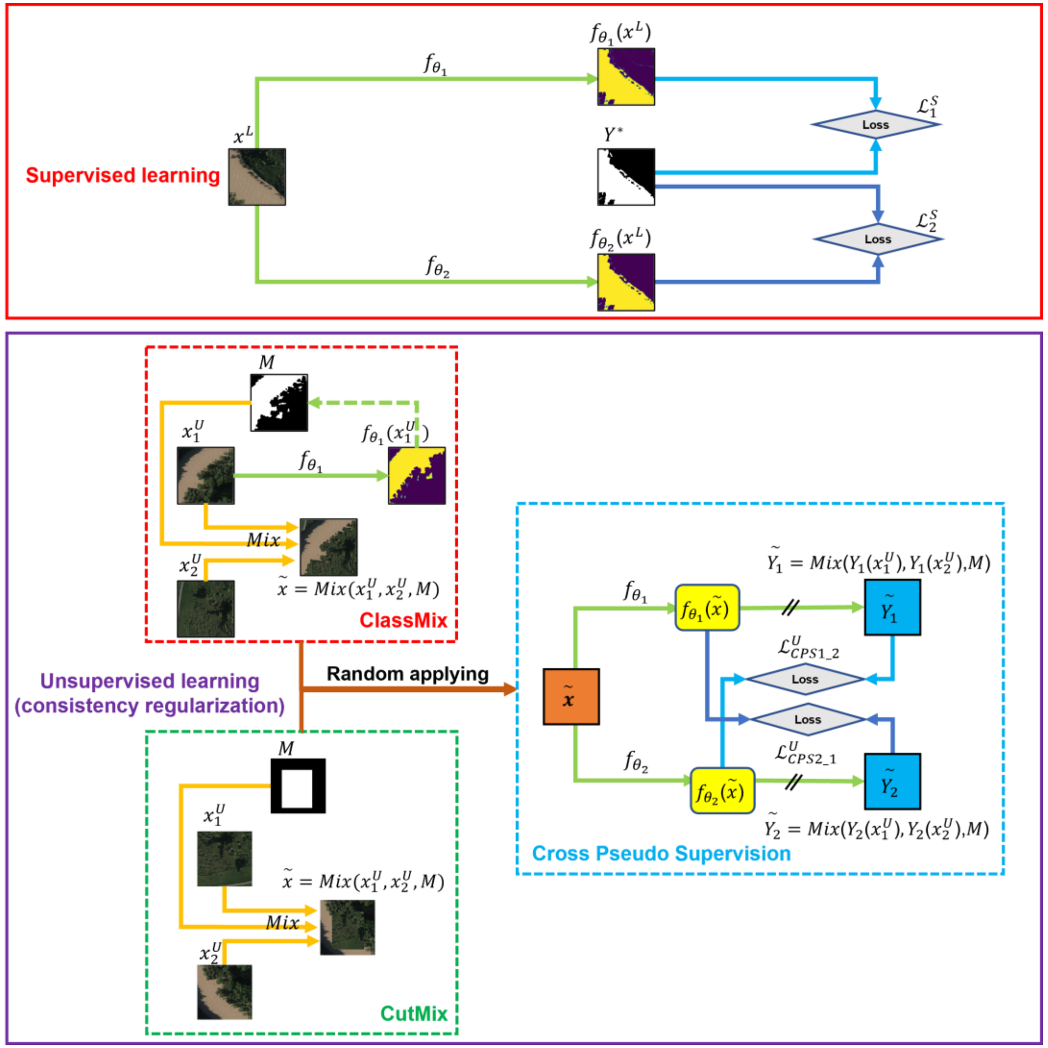

- x^L, x^U denote the labeled and unlabeled image, respectively, while Y^* denotes the ground truth label;
- f_{θ_1} and f_{θ_2} are two identical sub-models with different initialization parameters θ_1 and θ_2;
- $f_{\theta_1}(x^L)$ means the probability map of inputting image x^L to the model f_{θ_1};
- $Y_1(x_1^U)$ means the binarization map of inputting image x_1^U to the model f_{θ_1}, with a threshold of 0.5 (if probability >= 0.5, value = 1 → floodwater; otherwise, value = 0 → non-floodwater);
- $\tilde{x}$ is the mixed image based on the mask M generated based on CutMix or ClassMix strategy, while $\tilde{Y}_1$, $\tilde{Y}_2$ denote the mixed binarization maps using two unlabeled images and the same mask M;
- "//" signifies the stop-gradient.

Y. He, J. Wang, Y. Zhang, and C. Liao, "Enhancement of Urban Floodwater Mapping From Aerial Imagery With Dense Shadows via Semisupervised Learning," *IEEE Journal of Selected Topics in Applied Earth Observations and Remote Sensing*, pp. 9086-9101, 2022, doi: 10.1109/JSTARS.2022.3215730.

4. Experiments and results

- **Study area**

  - In June 2013, a major flooding hit the Calgary city, Canada.
  - The optical aerial imagery (0.2-m spatial resolution) was captured in the early morning (8:00-9:30 a.m.) on June 22, 2013, by the City of Calgary.
  - **Issue:** There are many shadows in the aerial imagery, leading to a large underestimation of extraction results.

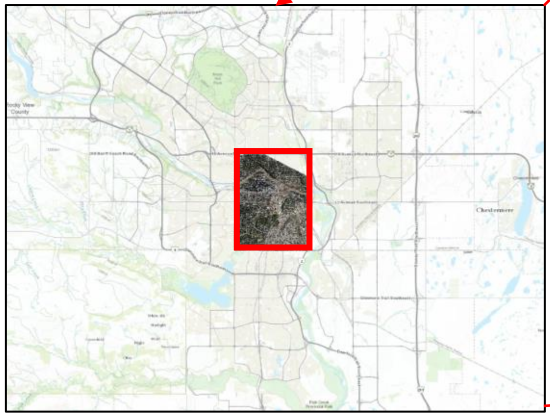

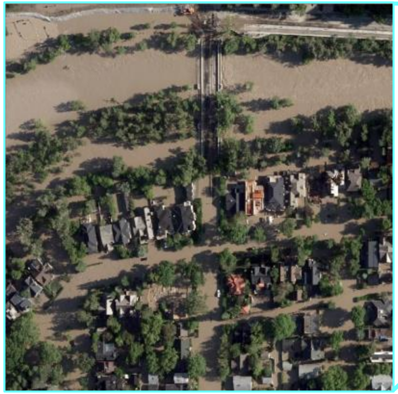

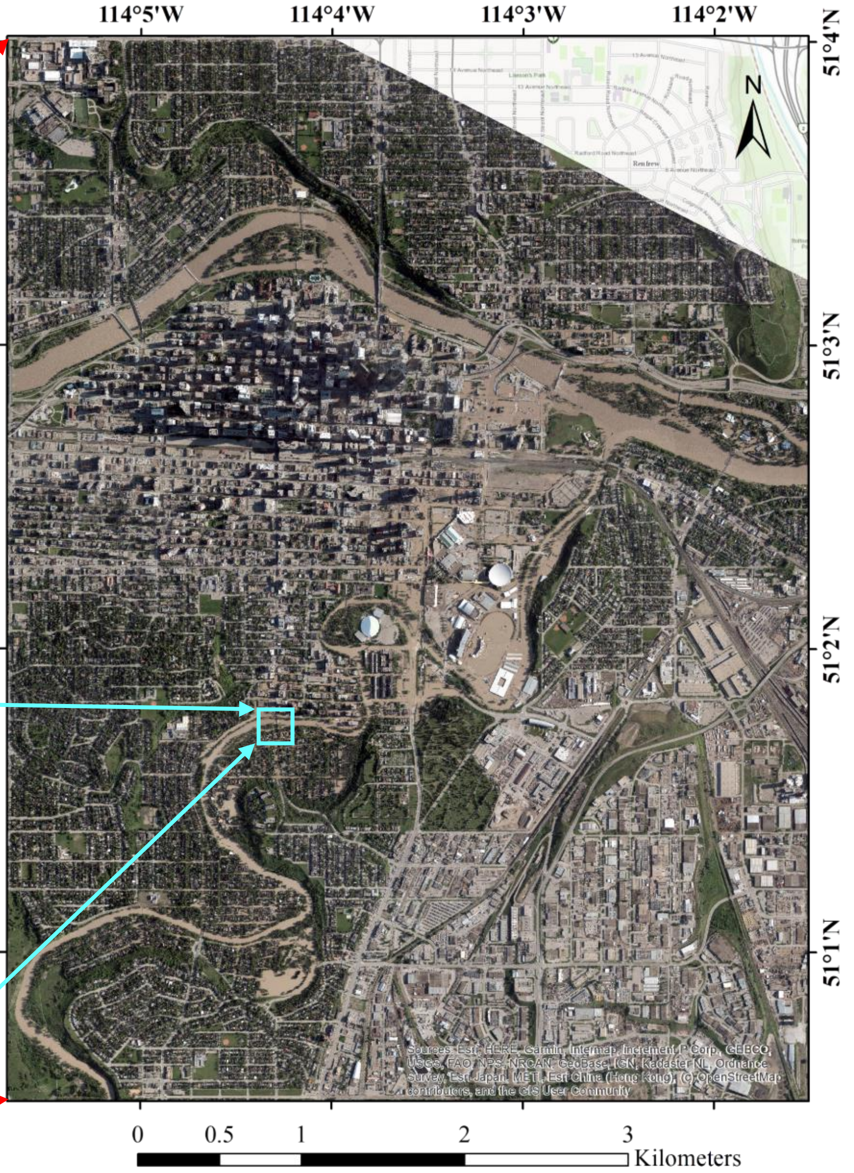

- **Data labeling**
  - ➢ The top left figure is the split grids. The whole area was split into 2048 × 2048-pixel small patches for collaborative labeling.
  - ➢ The top right figure is the final labeling results used as the ground truth data in the study.
  - ➢ Removing some invalid patches, we finally obtained 182 labeled patches without overlap.

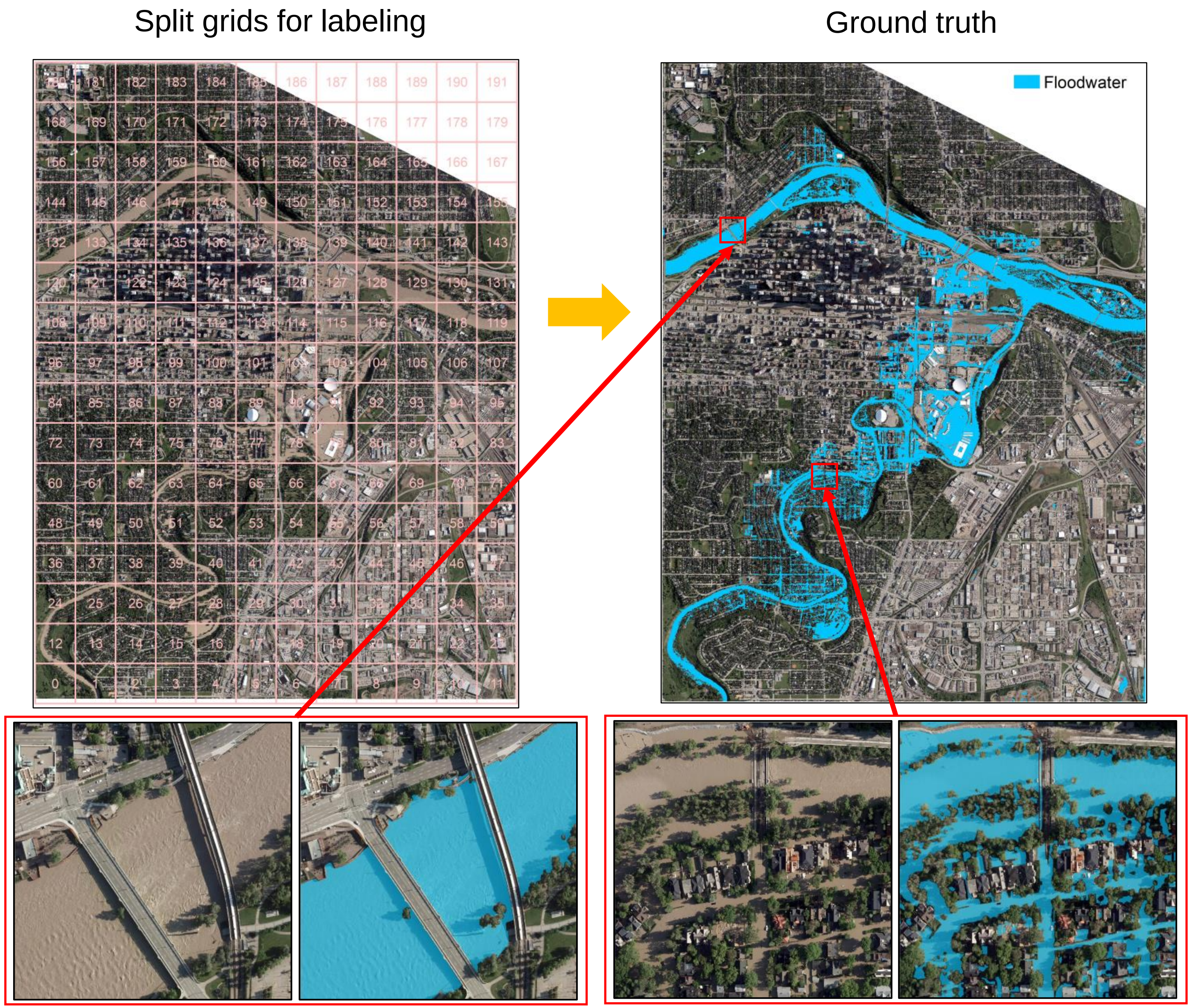

4. Experiments and results

- **Influence of shadows**

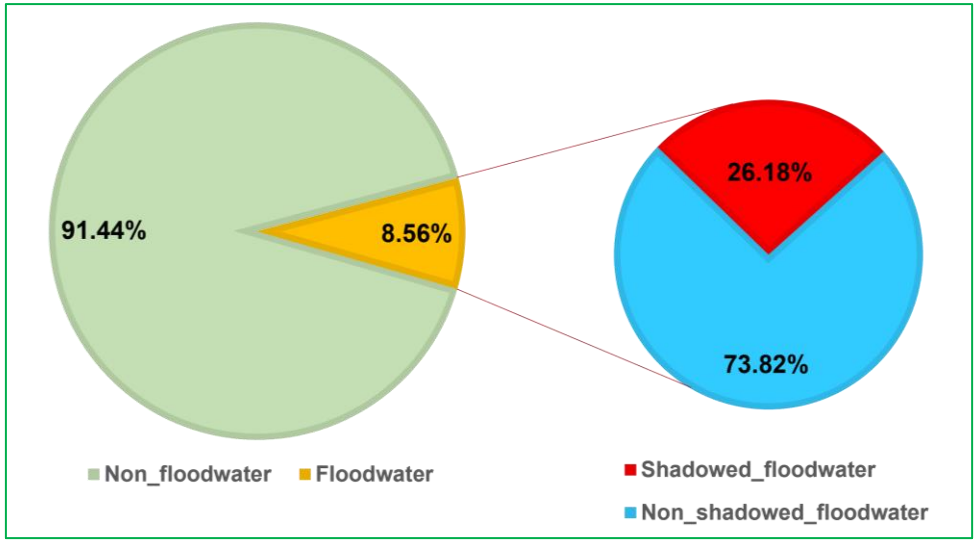

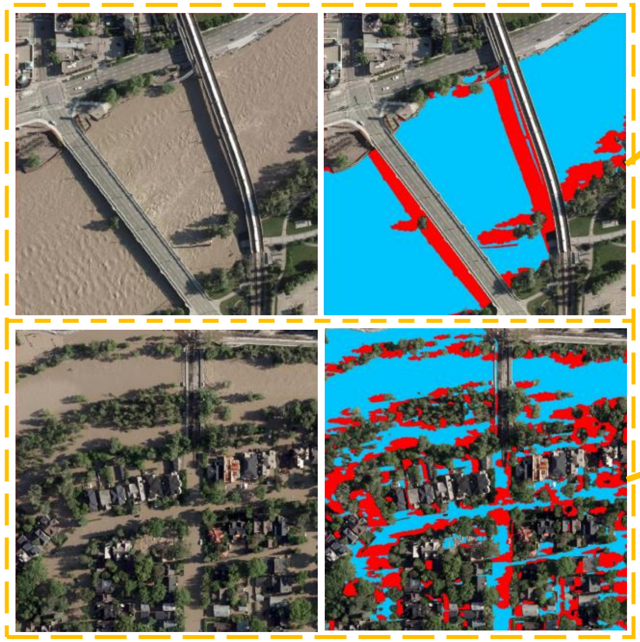

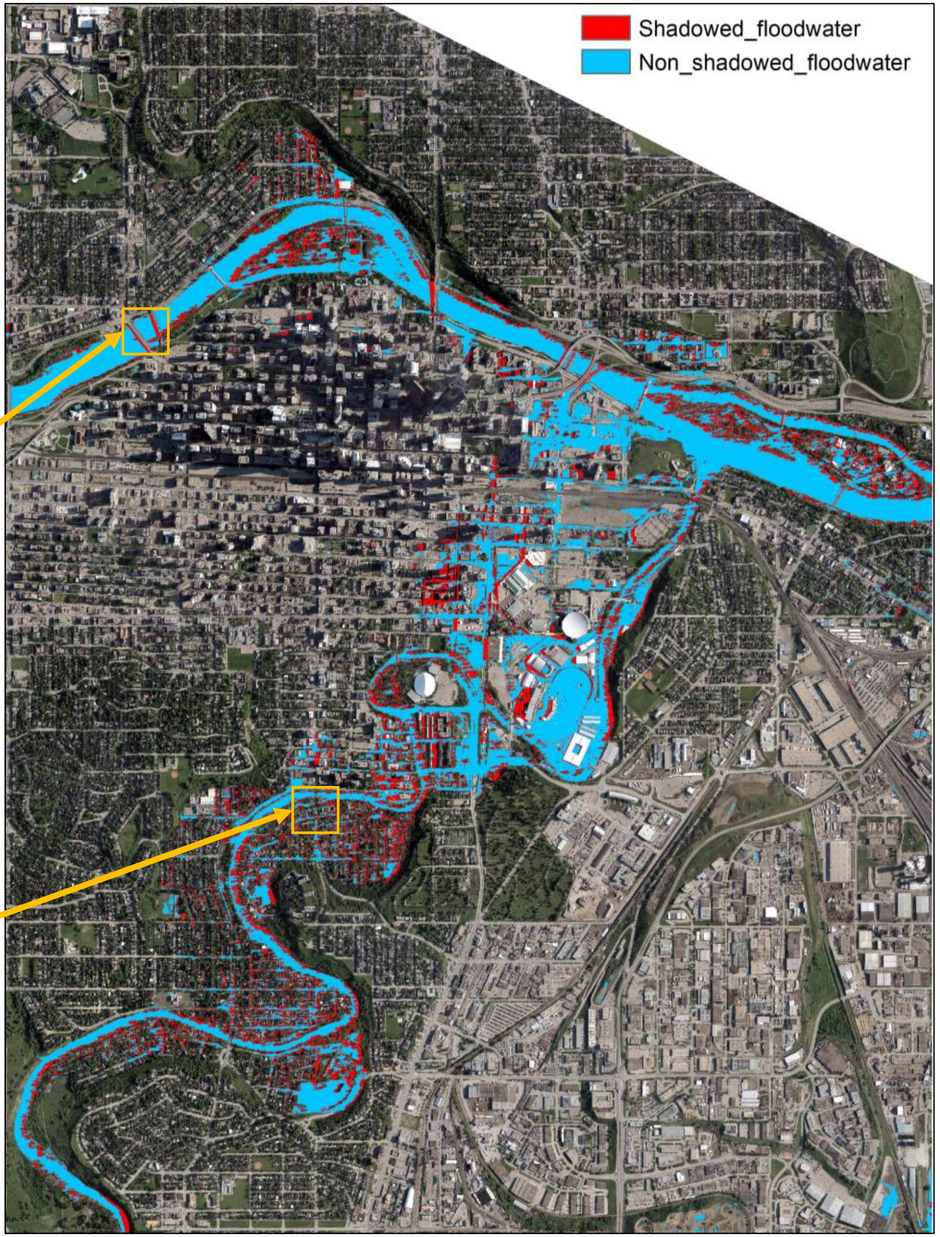

4. Experiments and results

- **Training sample selection**

  - **Two representative sites**

Site	Area (km²)	Land Use	Main Landscape
A	2.711	Central commercial area	Downtown center with high-rise buildings
B	2.681	Matured residential land	Matured residential area with single houses and trees

  - **Training data split**

	Training Stage		Evaluation Stage
	Training	Validation	Testing
Number of image patches	4	4	174
Patch size	2048×2048	2048×2048	2048×2048

As shown in the right image:

- The training samples are chosen from two representative sites A, and B.
- In training stage, total eight 2048×2048-pixel patches are used for training (patch id:13, 39, 102, 124) and validation (patch id: 14, 27, 125, 127).
- In evaluation stage, the remaining 174 patches are used to evaluate the model performance.
- The training samples used in training stage only account for 4.47% of the total data, the corresponding floodwater pixels account for 8.85% of the total floodwater.

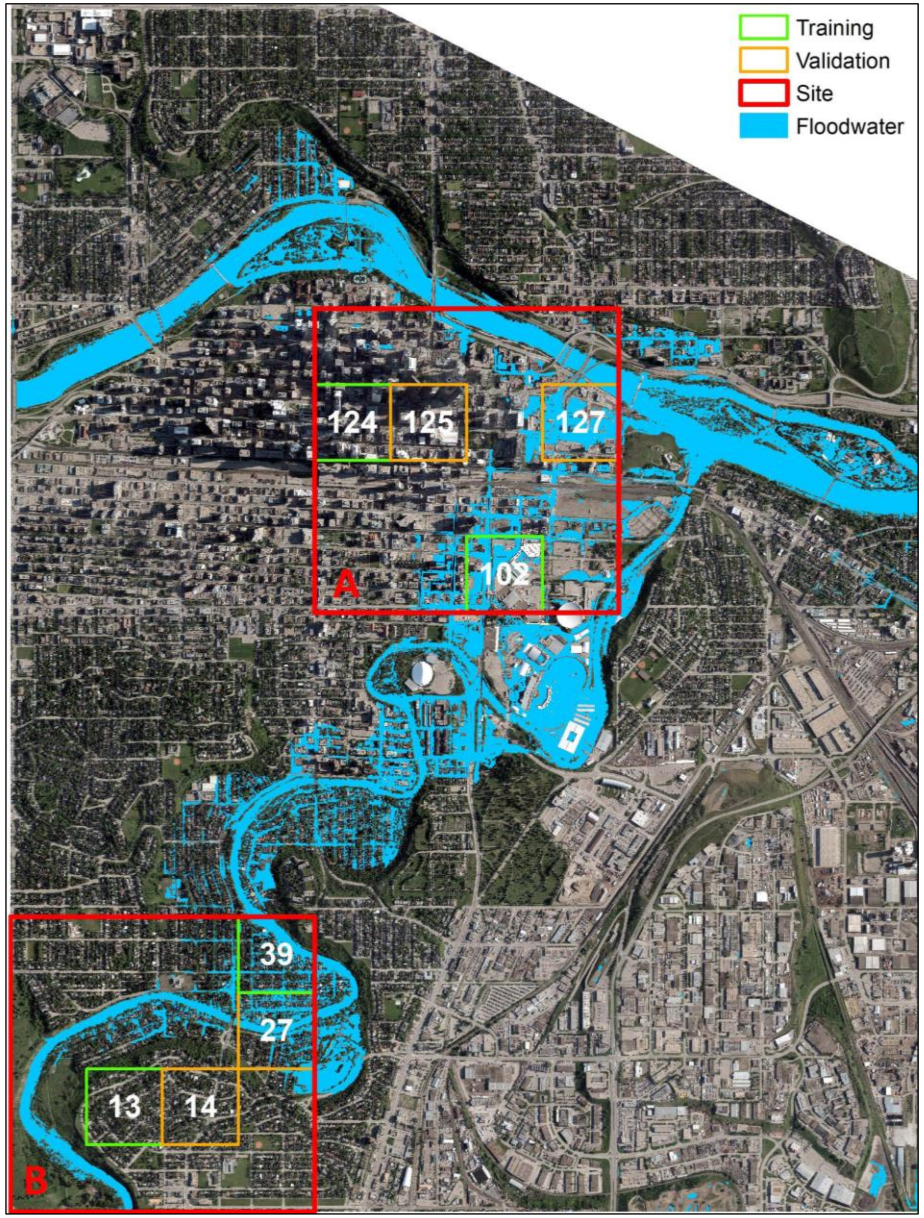

4. Experiments and results

- **Qualitative comparison**

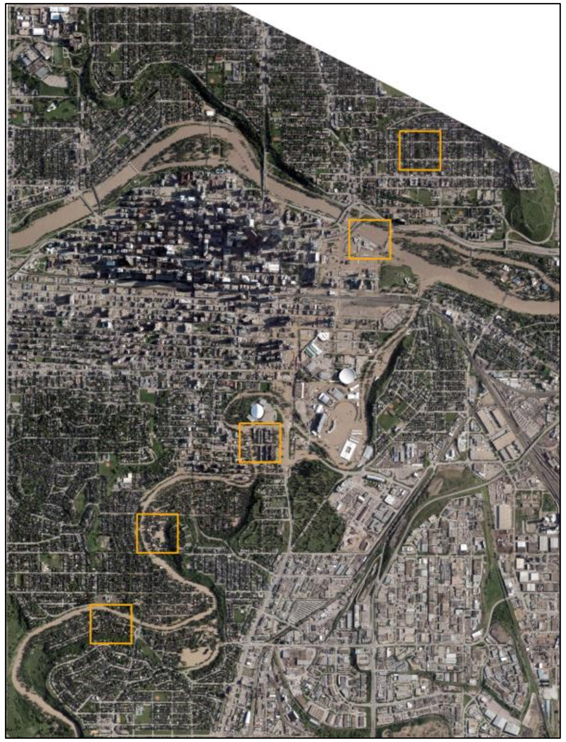

Image

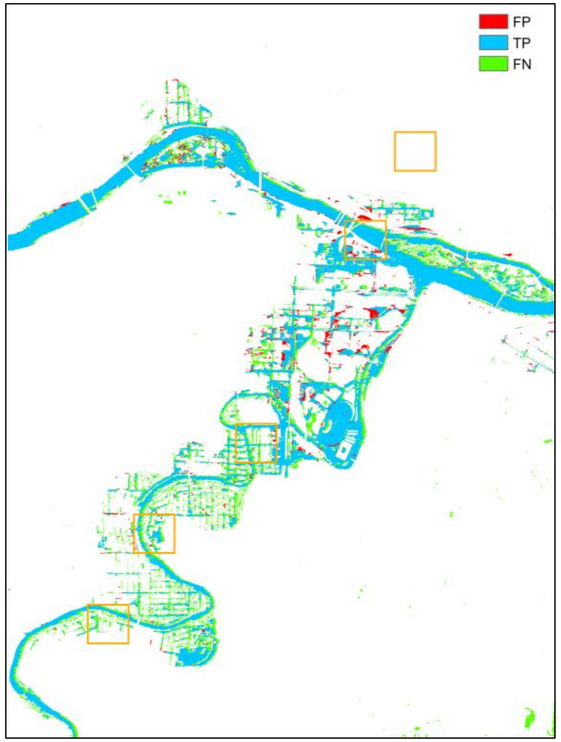

Floodwater index (FWI) (Zhang & Crawford, 2020)

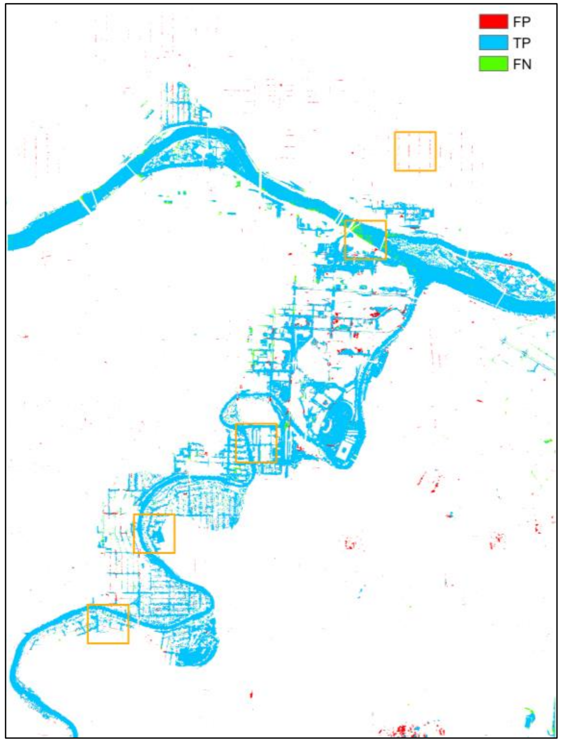

Supervised learning (SL)

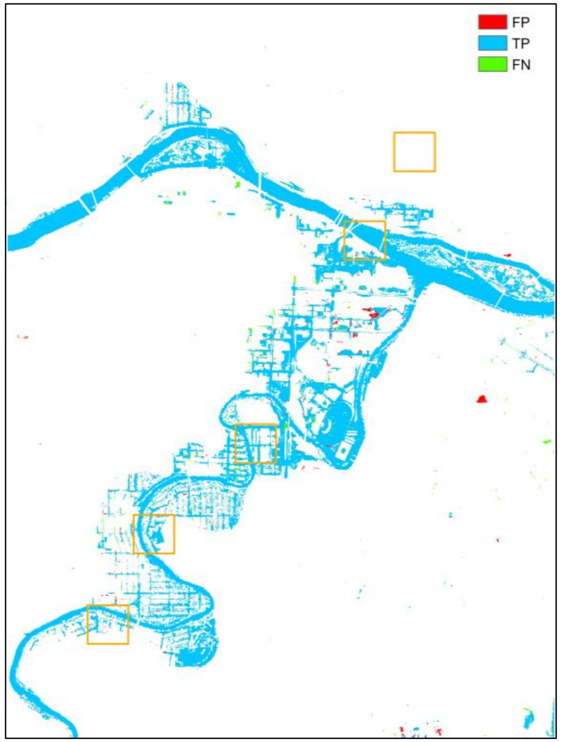

Semi-supervised learning (SSL)

FP is the incorrectly classified floodwater pixels

TP is the correctly classified floodwater pixels

FN is the missing floodwater pixels

- **Quantitative comparison**

Method		Precision	Recall	F1	IoU
FWI		90.63%	68.37%	77.94%	63.86%
Deep learning	SL	94.47%	92.99%	93.72%	88.19%
	SSL	**97.38%**	**95.31%**	**96.34%**	**92.93%**

4. Experiments and results

- **Enlarged examples**

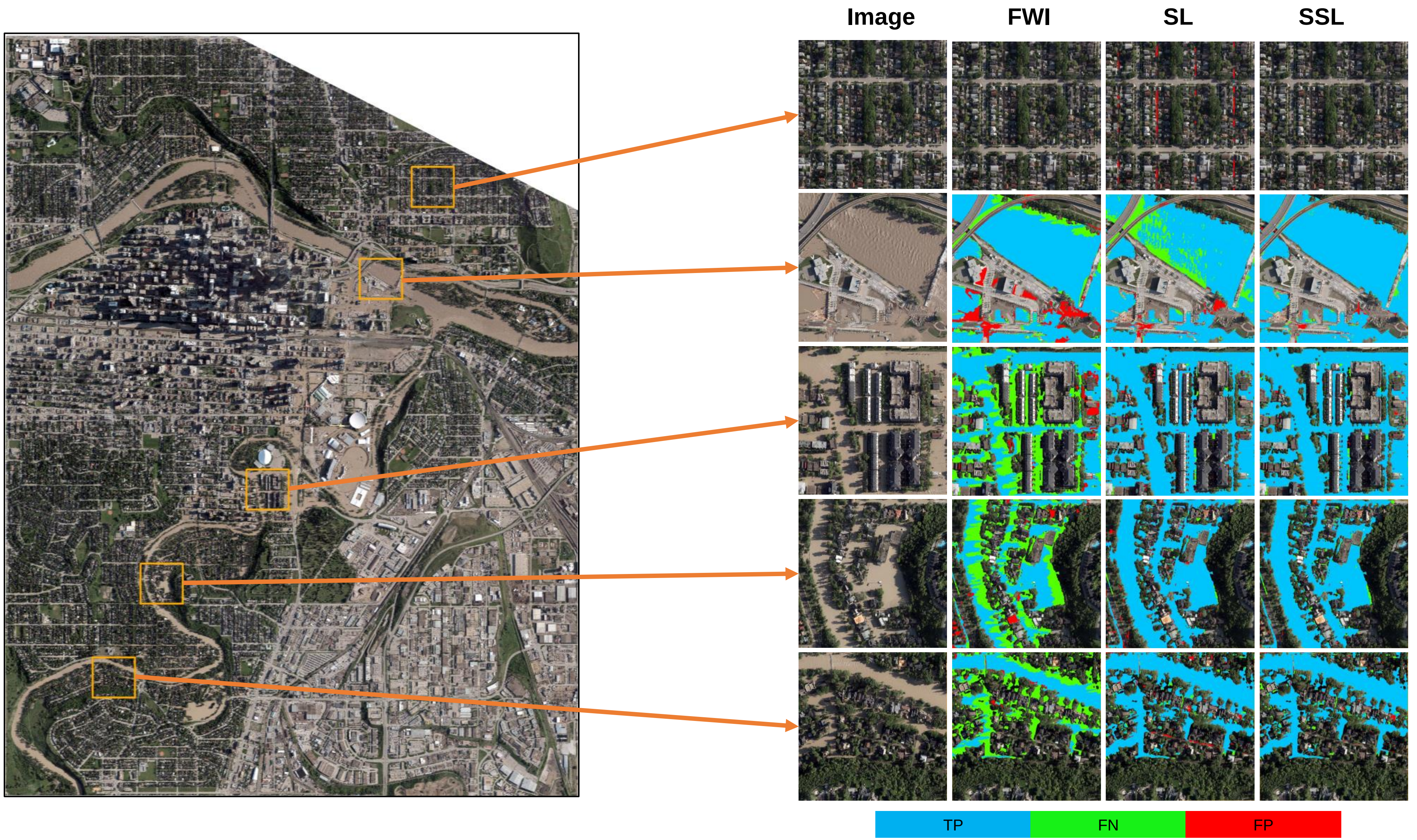

5. Conclusions

In this study:

- Shadow’s influence cannot be ignored in floodwater detection from dense urban areas.
- Deep learning methods can achieve much better results than traditional spectral index method due to considering the floodwater in shadows, despite much more training samples are required.
- Semi-supervised learning method can yield a remarkable performance (over 96% F1-score) only using a limited number of labeled samples (4.47% of the total data).

Future work:

- Investigating the performance of proposed method on multi-source and multi-modal remote sensing data.
- Exploring how to reduce the training cost facing a large amount of unlabeled data.

References

[1] C. Armenakis, E. X. Du, S. Natesan, R. A. Persad, and Y. Zhang, “Flood Risk Assessment in Urban Areas Based on Spatial Analytics and Social Factors,” *Geosciences*, vol. 7, no. 4, Art. no. 4, Dec. 2017, doi: 10.3390/geosciences7040123.

[2] Q. Feng, J. Liu, and J. Gong, “Urban Flood Mapping Based on Unmanned Aerial Vehicle Remote Sensing and Random Forest Classifier—A Case of Yuyao, China,” *Water*, vol. 7, no. 4, Art. no. 4, Apr. 2015, doi: 10.3390/w7041437.

[3] S. Ghaffarian, N. Kerle, and T. Filatova, “Remote Sensing-Based Proxies for Urban Disaster Risk Management and Resilience: A Review,” *Remote Sensing*, vol. 10, no. 11, p. 1760, Nov. 2018, doi: 10.3390/rs10111760.

[4] X. Shen, D. Wang, K. Mao, E. Anagnostou, and Y. Hong, “Inundation Extent Mapping by Synthetic Aperture Radar: A Review,” *Remote Sensing*, vol. 11, no. 7, Art. no. 7, Jan. 2019, doi: 10.3390/rs11070879.

[5] Y. Zhang and P. Crawford, “Automated Extraction of Visible Floodwater in Dense Urban Areas from RGB Aerial Photos,” *Remote Sensing*, vol. 12, no. 14, Art. no. 14, Jan. 2020, doi: 10.3390/rs12142198.

[6] Y. He, J. Wang, Y. Zhang, and C. Liao, “Enhancement of Urban Floodwater Mapping From Aerial Imagery With Dense Shadows via Semisupervised Learning,” *IEEE Journal of Selected Topics in Applied Earth Observations and Remote Sensing*, vol. 15, pp. 9086–9101, 2022, doi: 10.1109/JSTARS.2022.3215730.

Acknowledgement

- City of Calgary
- Natural Resources Canada
- NSERC
- Dr. Jinfei Wang (Supervisor)
- Dr. Ying Zhang (Co-supervisor)

Thanks

yhe563@uwo.ca